



# A pure neural network controller for double-pendulum crane anti-sway control: Based on Lyapunov stability theory

Qingrong Chen<sup>1,2,3</sup> | Wenming Cheng<sup>1,2</sup> | Lingchong Gao<sup>3</sup> | Johannes Fottner<sup>3</sup>

<sup>1</sup>School of Mechanical Engineering,  
Southwest Jiaotong University, Sichuan,  
China

<sup>2</sup>Technology and Equipment of Rail  
Transit Operation and Maintenance Key  
Laboratory of Sichuan Province, Sichuan,  
China

<sup>3</sup>Department of Mechanical Engineering,  
Technical University of Munich, Bayern,  
Germany

## Correspondence

Wenming Cheng, No. 111, North 1st  
Section, 2nd Ring Road, Chengdu 610031,  
Sichuan, China.

Email: [wmcheng@home.swjtu.edu.cn](mailto:wmcheng@home.swjtu.edu.cn)

## Funding information

China Scholarship Council, Grant/Award  
Number: 201807000126; Sichuan Province  
Science and Technology Program, Grant/  
Award Numbers: 2019YFG0300 and  
2019YFG0285

## Abstract

Crane systems have been widely applied in logistics due to their efficiency of transportation. The parameters of a crane system may vary from each transport, therefore the anti-sway controller should be designed to be insensitive to the variation of system parameters. In this paper, we focus on pure neural network adaptive tracking controller design issue that does not require the parameters of crane systems, i.e. the trolley mass, the payload mass, the cable lengths, and etc. The proposed neural network controller only requires the output feedback signals of the trolley, i.e. the position and the velocity, which means no sway measuring equipment is needed. The Lyapunov method is utilized to design the weights update law of neural network, and the robustness of the proposed controller is proved by the Lyapunov stability theory. The results of numerical simulations show that the proposed neural network controller has excellent performance of trolley position tracking and payload anti-sway controlling.

## KEYWORDS

adaptive control, anti-sway control, double-pendulum crane systems, Lyapunov stability theory, neural network control

## 1 | INTRODUCTION

Crane systems with cable hoisting mechanism are typically under-actuated systems. They play an important role in logistics and are widely used in container harbors, railway container yards, and other industrial factories. As cable hoisting mechanism is adopted, the weight of the crane is reduced, but the payload swings unavoidably during the transportation as well as reaching the desired position. The sway of the payload decreases the efficiency of crane's transportation and may result in hazards, such as collision, tip over, and etc. To improve the effectiveness and the safety of crane, researchers proposed many

anti-sway control strategies to position the trolley accurately and eliminate the payload sway. All the anti-sway control strategies aim to: i) move the trolley safely, fast, and accurately to the desired position, and ii) decrease the sway of the payload as much as possible during the transportation and eliminate the residual sway when reaching the desired position.

If the parameters of crane systems are exactly known, open-loop control strategies can work effectively. Singhow et al. reviewed the command shaping/input shaping [1] and implemented the method on double-pendulum crane systems [2,3]. It shows that the method can eliminate the payload sway effectively and is even

faster than feedback controllers. However, it cannot resist external disturbances and is sensitive to the variation of system parameters. To reject the external disturbances, hybrid controllers consisted of PID feedback control and input shaping are proposed for single-pendulum [4] and double-pendulum systems [5]. The feedback module is used for the disturbances rejecting and trolley positioning, and input shaping is used to reduce the motion-induced the payload sway. Note that all the aforementioned controllers require retuning/retraining the control parameters carefully when the parameters of crane system change. To improve the robustness to the variation of system parameters, Jaafar et al. [6] proposed a model reference command shaping approach without the prior knowledge of the system frequency and damping ratio, and implemented it on a double pendulum crane system. The method's weakness is that the residual sway angles of the hook and the payload are approximately 1~2 degrees. Maghsoudi et al. [7] proposed an improved unity magnitude zero vibration shaper whose parameters are automatically chosen by a PSO tuner without using the natural frequencies and damping ratios of the overhead crane.

For crane systems with uncertain/unknown parameters, which are more similar to actual engineering as the payload mass and cable length vary from transport to transport, we need a controller which is insensitive to the changes of system parameters or even model-free. Many researchers proposed regulation controllers to concurrently achieve precise trolley positioning and fast payload swing eliminating. Lu et al. [8] proposed an enhanced-coupling adaptive controller with an adaption law which is designed to identify the uncertain payload mass. Sun et al. [9] designed an adaptive model-free anti-swing control strategy with an adaption law to online estimate uncertain friction. An enhanced coupling nonlinear control method [10], two sliding mode control (SMC)-based strategies [11] and a novel amplitude-saturated output feedback control approach without velocity signals [12] are robust to variation of system parameters but require the nominal values of them. Model-free control strategies [13,14] are designed to improve the robustness w.r.t uncertain parameters, such as payload mass and cable lengths. Ngo et al. [15] proposed an adaptive-gain SMC with a prediction mechanism to estimate the external disturbances. The aforementioned control strategies of this paragraph require full states feedback. However, in practical applications, the swing angles of the hook and the payload are difficult to obtain, thus the strategies are limited for the real applications. Fortunately, tracking control works well even if only partial feedback, such as the output feedback signals from the trolley, is available. It is a great advantage

compared to regulation control which requires full states feedback. Trajectory plan methods [16,17] that applied in double-pendulum crane can effectively decrease both the payload and the hook sway. We find that the trajectories can be designed to be conservative so that they are robust to the changes of the cable lengths and the payload mass. Then, by designing a trajectory tracking controller, the sways will be eliminated when the tracking performance is perfect.

Since the artificial intelligence methods, such as Fuzzy, Neural Network (NN), Particle Swarm Optimization (PSO), and etc., are widely studied and used, we consider that it is necessary to open a new paragraph to illustrate the intelligent control schemes which are implemented in the field of crane control problems. We can utilize intelligent methods to improve the conventional control schemes, such as PID, SMC and/or other controllers. Choi et al. [18] and Suh et al. [19] used offline pre-trained NN self-tuner to tune PID parameters online. The results show that the controller retains the advantages of the PID controller, and improves the robustness to parameters variation and external disturbances. Saeidi et al. [20] proposed an input shaping-inspired offline training algorithm to train a NN PID controller which is combined with feedback control. Jaafar et al. [21] proposed a PID controller whose control gains are offline tuned by using PSO algorithm. The controller requires exact parameters of the system, and the control gains need to be re-tuned once the parameters vary. Shehu et al. [22] proposed a novel SMC tuned by NN and Fuzzy algorithm. The intelligent strategies in the aforementioned intelligent controllers of this paragraph are pre-trained offline before simulation or implementation. Shao et al. [23] proposed a Fuzzy model and PSO-based LQR anti-sway controller, in which PSO is used to choose the LQR weight matrices. Lee et al. [24] put forward an SMC-based training algorithm to train the NN controller and Frikha et al. [25] proposed a radial basis function neural network (RBFNN)-based adaptive neuro-sliding mode controller with full states feedback. These controllers are robustness to the variation of system parameters and behave good anti-sway performance. However, except [22,25], other controllers do not prove the stability in the sense of Lyapunov. Different from the aforementioned intelligent controllers, [26] proposed a regulation controller with a NN friction compensator without prior knowledge of friction characteristics and is tested on a self-built 3D tower crane testbed, [27–30] utilized RBFNN to estimate/compensate unknown dynamics, and [31] proposed an RBFNN controller to deal with a class of nonlinear systems with unknown parameters.

There are two motivations of this paper: i) according to the existing references, we found that NN can be used to

approximate any unknown functions, so we believe that it is possible to design a NN controller to approximate the ideal control law of the crane systems, and ii) the sway angles of the hook and the payload are difficult to measure fast and accurately in the practical applications, however, tracking controllers can work well without these signals, so we can design a tracking controller to solve the anti-sway problem of crane systems. Combining these two motivations, we proposed a pure NN controller (PNNC) to solve the anti-sway problem and the positioning problem concurrently by tracking the ideal trajectory of the trolley.

In this paper, we choose a similar Lyapunov function as in [27], but we design a novel control law which is the output of a NN. The Lyapunov method is utilized to design NN weights update law, and the robustness of the proposed controller is proved by the Lyapunov stability theory. Finally, we run several numerical simulations to validate the tracking performance and the sway eliminating performance of the proposed controller.

The rest of this paper is organized as follows. In Section 2, the dynamic equations of under-actuated crane systems are provided. Then, we illustrate the choice of control law, weights update law, as well as stability analysis in Section 3 in detail. In Section 4, several numerical simulations are conducted to verify the tracking performance of the proposed approach. Finally, some conclusions are given in Section 5.

## 2 | DOUBLE-PENDULUM CRANE DYNAMICS

The planar model of a 2-D double-pendulum overhead crane is shown in Figure 1.  $m_t$ ,  $m_h$ , and  $m_p$  denote the trolley mass, the hook mass, and the payload mass respectively,  $l_1$  and  $l_2$  denote the cable lengths,  $u$  denotes the control force,  $x$  denotes the trolley displacement,  $\alpha$  and  $\beta$  denote the hook sway angle and the payload sway angle with respect to the vertical.

Several assumptions are given as follows:

- i). the deflection of the crane structure can be ignored.
- ii). the payload and the hook are both considered as mass points.
- iii). the damping effect of the trolley running friction and the air resistance of the payload are ignored, and there is no random external disturbance.
- iv). the cable is massless and the cable length is considered as constant.
- v). both the hook and the payload swing near the equilibrium point.

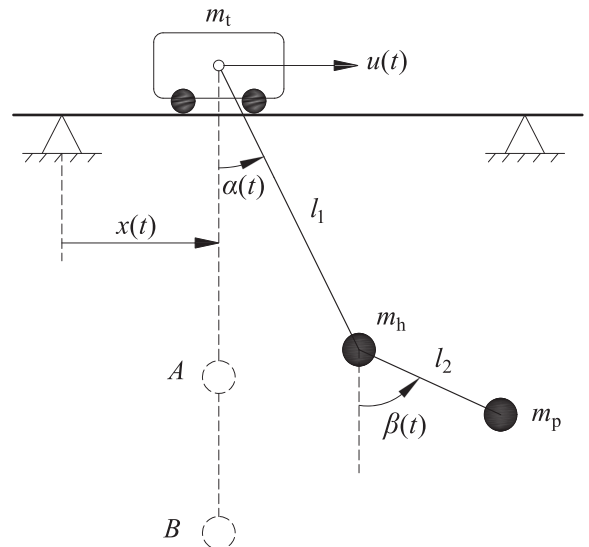


**FIGURE 1** Simplified schematic diagram of planar double-pendulum overhead crane

Lagrange's equations are widely used to establish multi-bodies dynamics function. Given generalized coordinates  $\mathbf{q}$ , generalized forces  $\mathbf{Q}$  and Lagrangian function  $\mathcal{L}$ , the Lagrange's equations are defined as

$$\frac{d}{dt} \left( \frac{\partial \mathcal{L}}{\partial \dot{q}_i} \right) - \frac{\partial \mathcal{L}}{\partial q_i} = Q_i \quad (1)$$

where  $i=1,2,\dots,N$  labels the generalized coordinates, and  $\mathcal{L} = T - V$ , in which  $T$  and  $V$  denote the kinetic energy and potential energy of the dynamic system respectively. As shown in Figure 1, we can choose generalized coordinates  $\mathbf{q}=[q_1, q_2, q_3]^T=[x, \alpha, \beta]^T$  and generalized forces  $\mathbf{Q}=[Q_1, Q_2, Q_3]^T=[u, 0, 0]^T$ . The kinetic energy is

$$\begin{aligned} T &= \frac{1}{2}m_t\dot{x}^2 + \frac{1}{2}m_h \left[ [l_1\dot{\alpha}\cos\alpha + \dot{x}]^2 + [l_1\dot{\alpha}\sin\alpha]^2 \right] \\ &\quad + \frac{1}{2}m_p \left[ [l_2\dot{\beta}\cos\beta + l_1\dot{\alpha}\cos\alpha + \dot{x}]^2 \right. \\ &\quad \left. + l_2\dot{\beta}\sin\beta + l_1\dot{\alpha}\sin\alpha \right]^2 \\ &= \frac{1}{2}m_t\dot{x}^2 + \frac{1}{2}(m_h + m_p) \left[ l_1^2\dot{\alpha}^2 + \dot{x}^2 + 2l_1\dot{x}\dot{\alpha}\cos\alpha \right] \\ &\quad + \frac{1}{2}m_p \left[ l_2^2\dot{\beta}^2 + 2l_1l_2\dot{\alpha}\dot{\beta}\cos[\alpha - \beta] + 2l_2\dot{x}\dot{\beta}\cos\beta \right] \end{aligned} \quad (2)$$

Consider the equilibrium the position of the payload (point B in Figure 1) as the zero potential energy point, therefore we can derive the potential energy of the system

$$\begin{aligned}
V &= m_{tg}(l_1 + l_2) + m_{hg}(l_1 - l_1 \cos\alpha + l_2) \\
&\quad + m_pg(l_1 - l_1 \cos\alpha + l_2 - l_2 \cos\beta) \\
&= (m_t + m_h + m_p)(l_1 + l_2)g - (m_h + m_p)gl_1 \cos\alpha \\
&\quad - m_pg l_2 \cos\beta
\end{aligned} \tag{3}$$

With equation (1)-(3), the double-pendulum crane nonlinear dynamics equations then can be derived as follows

$$\left\{
\begin{array}{l}
\ddot{x}\{m_t + m_h + m_p + m_p l_2\}[\ddot{\beta} \cos\beta - \dot{\beta}^2 \sin\beta + l_1\{m_h + m_p\}(\ddot{\alpha} \cos\alpha - \dot{\alpha}^2 \sin\alpha) = u \\
l_1\{m_h + m_p\}[\ddot{x} \cos\alpha + l_1 \ddot{\alpha} + g \sin\alpha + m_p l_1 l_2 [\ddot{\beta} \cos(\alpha - \beta) + \dot{\beta}^2 \sin(\alpha - \beta)] = 0 \\
m_p l_2 [\ddot{x} \cos\beta + l_1 \ddot{\alpha} \cos(\alpha - \beta) + l_2 \ddot{\beta} - l_1 \dot{\alpha}^2 \sin(\alpha - \beta) + g \sin\beta] = 0.
\end{array}
\right. \tag{4}$$

With the assumption v), we have

$$\left\{
\begin{array}{l}
\sin\alpha \approx \alpha, \cos\alpha \approx 1, \sin\beta \approx \beta, \cos\beta \approx 1 \\
\sin(\alpha - \beta) \approx \alpha - \beta, \cos(\alpha - \beta) \approx 1 \\
\dot{\alpha}^2 \approx 0, \dot{\beta}^2 \approx 0.
\end{array}
\right. \tag{5}$$

then nonlinear dynamic equations equation (4) can be simplified to linear dynamic equations, and we divide the simplified equations into two subsystems:  $x$ -subsystem

$$\ddot{x} = \frac{m_h + m_p}{m_t} g \alpha + \frac{1}{m_t} u \tag{6}$$

and  $\alpha\beta$ -subsystem

$$\left\{
\begin{array}{l}
\ddot{\alpha} = -\frac{1}{l_1} \left( \ddot{x} + \frac{m_h + m_p}{m_h} g \alpha - \frac{m_p}{m_h} g \beta \right) \\
\ddot{\beta} = \frac{g}{m_h l_2} (m_h + m_p) (\alpha - \beta).
\end{array}
\right. \tag{7}$$

### 3 | CONTROLLER DESIGN AND ANALYSIS

#### 3.1 | RBFNN

Inspired by [27,31], here we proposed a novel pure RBFNN adaptive tracking controller which is utilized to control the trolley's the position. RBFNN has 3 layers: input layer, hidden layer, and output layer, see Figure 2. The hidden-layer activation functions are radial basis functions, and each neuron in this layer include a central

vector  $\mathbf{c}_j$  whose dimension is the same as NN input vector  $\mathbf{X}$ . The Euclidean distance of  $\mathbf{c}_j$  and  $\mathbf{X}$  is defined as  $\|\mathbf{X} - \mathbf{c}_j\|$ . The expression of RBFNN can be written as

$$\begin{cases} \varphi_j = \exp\left(-\left(\|\mathbf{X} - \mathbf{c}_j\|^2\right)/\left(2b_j^2\right)\right), & j = 1, 2, \dots, m \\ \mathbf{y} = \theta^T \varphi \end{cases} \tag{8}$$

where  $\mathbf{c}_j$  is the central vector of  $j^{\text{th}}$  hidden-layer neuron, positive scalar  $b_j$  represents the width of  $j^{\text{th}}$  hidden-layer

neuron,  $\varphi = [\varphi_1, \varphi_2, \dots, \varphi_m]^T$  represents hidden-layer output vector,  $\theta$  is the weights matrix/vector of RBFNN, and  $y$  is the final output of RBFNN.

#### 3.2 | Choice of Control Law

In this section, the control law of the PNCC will be designed. Here we only need the output parameters of the trolley, i.e. the position and the velocity. This means the output parameters of the hook and the payload, i.e.

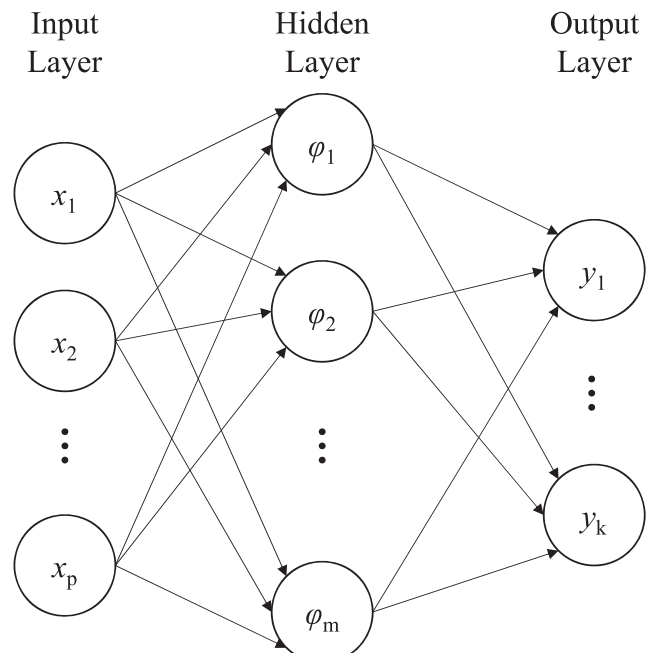


**FIGURE 2** Architecture of RBFNN

the sway angle and the sway velocity, are not required. As a result, no swing measuring equipment is required. Dealing with a nonlinear model of a crane is complicated, therefore, we utilize the simplified linear model (6) to design the control law and update law. This method was adopted in [32,33], too. Here we rewrite equation (6) as

$$\ddot{x} = f + \frac{1}{m_t} u \quad (9)$$

where  $f = \frac{m_h + m_p}{m_t} g \alpha$ .

The trolley's the position tracking error is defined as

$$e = x_d - x \quad (10)$$

where  $x$  and  $x_d$  denote the trolley's actual the position and its ideal the position, respectively. Then we can derive the trolley's the velocity tracking error

$$\dot{e} = \dot{x}_d - \dot{x} \quad (11)$$

where  $\dot{x}$  and  $\dot{x}_d$  denote the trolley's actual velocity and its ideal velocity, respectively.

Suppose that both the trolley mass  $m_t$  and function  $f$  are known exactly. Applying model-reference adaptive control (MRAC) method [34], one can design the ideal control law, based equation (9), as

$$u^* = -m_t [f - [\ddot{x}_d + \kappa^T \epsilon]] \quad (12)$$

where  $\ddot{x}_d$  denotes the trolley's ideal acceleration,  $\epsilon^T = [e, \dot{e}]$ , and  $\kappa^T = [k_p, k_d]$  with  $k_p$  represents proportional control gain,  $k_d$  represents differential control gain, and  $k_p = 2\sqrt{k_d}$ .

However, as the trolley mass  $m_t$ , the hook mass  $m_h$ , the payload mass  $m_p$ , and the sway angle  $\alpha$  are unknown and/or unmeasurable in the practical application, function  $f$  is unknown, therefore, the control law (12) can be hardly designed. Combining with equation (8), we choose the control law of the PNNC as

$$u = -y = -\theta^T \varphi \quad (13)$$

### 3.3 | Choice of Weights Update Law and Stability Analysis

To achieve  $\ddot{x} = \ddot{x}_d$ , assume that the NN weights from hidden layer to output layer are the optimal weights, denoted as  $\theta^*$ . Combining equation (12) and equation (13), we have

$$-m_t [f - [\ddot{x}_d + \kappa^T \epsilon]] = -\theta^{*T} \varphi + \Delta \quad (14)$$

where  $\Delta$  is the PNNC approximation error, we then obtain

$$f = \frac{1}{m_t} (\theta^{*T} \varphi - \Delta) + \ddot{x}_d + \kappa^T \epsilon \quad (15)$$

By substituting the control law (13) into (9), one can derive

$$\ddot{x} = f - \frac{1}{m_t} y \quad (16)$$

Combining with (15), the acceleration tracking error is obtained as follow

$$\begin{aligned} \ddot{e} &= \ddot{x}_d - \ddot{x} = \ddot{x}_d - \left( f - \frac{1}{m_t} y \right) \\ &= \ddot{x}_d - \left[ \frac{1}{m_t} [\theta^{*T} \varphi - \Delta] + \ddot{x}_d + \kappa^T \epsilon - \frac{1}{m_t} \theta^T \varphi \right] \\ &= \frac{1}{m_t} (\theta - \theta^*)^T \varphi - \kappa^T \epsilon + \frac{1}{m_t} \Delta \end{aligned} \quad (17)$$

Define that

$$\mathbf{A} = \begin{bmatrix} 0 & 1 \\ -k_p & -k_d \end{bmatrix}, \mathbf{B} = \begin{bmatrix} 0 \\ 1 \end{bmatrix} \quad (18)$$

Equation (17) can be rewritten as

$$\dot{\epsilon} = \mathbf{A} \epsilon + \mathbf{B} Z \quad (19)$$

where  $\dot{\epsilon}^T = [\dot{e}, \ddot{e}]$ , and  $Z = \frac{1}{m_t} (\theta - \theta^*)^T \varphi + \frac{1}{m_t} \Delta$ .

Consider the globally positive definite Lyapunov function candidate

$$L = \frac{1}{2} \epsilon^T \Phi \epsilon + \frac{1}{2\gamma m_t} (\theta - \theta^*)^T (\theta - \theta^*) \quad (20)$$

where  $\gamma$  is a positive constant, and  $\Phi$  is a symmetric positive definite constant matrix.  $\Phi$  satisfies

$$-\Theta = \mathbf{A}^T \Phi + \Phi \mathbf{A} \quad (21)$$

for a chosen symmetric positive definite constant matrix  $\Theta$ .

Define that  $L_1 = \frac{1}{2} \epsilon^T \Phi \epsilon$  and  $L_2 = \frac{1}{2\gamma m_t} (\theta - \theta^*)^T (\theta - \theta^*)$ .

The first order time derivative of  $L_1$  and  $L_2$  can be calculated as follows [27]

$$\dot{L}_1 = -\frac{1}{2} \epsilon^T \Theta \epsilon + \epsilon^T \Phi \mathbf{B} Z \quad (22)$$

$$\dot{L}_2 = \frac{1}{\gamma m_t} (\theta - \theta^*)^T \dot{\theta} \quad (23)$$

Both  $\epsilon^T \Phi B$  and  $(\theta - \theta^*)^T \varphi$  are  $1 \times 1$  dimension matrices, therefore  $\epsilon^T \Phi B (\theta - \theta^*)^T \varphi = (\theta - \theta^*)^T \varphi \epsilon^T \Phi B$ . Substitute  $Z$  into equation (22) to derive

$$\begin{aligned}\dot{L}_1 &= -\frac{1}{2} \epsilon^T \Theta \epsilon + \frac{1}{m_t} \epsilon^T \Phi B (\theta - \theta^*)^T \varphi + \frac{1}{m_t} \epsilon^T \Phi B \Delta \\ &= -\frac{1}{2} \epsilon^T \Theta \epsilon + \frac{1}{m_t} (\theta - \theta^*)^T \varphi \epsilon^T \Phi B + \frac{1}{m_t} \epsilon^T \Phi B \Delta \quad (24)\end{aligned}$$

We then obtain

$$\begin{aligned}\dot{L} &= \dot{L}_1 + \dot{L}_2 \\ &= -\frac{1}{2} \epsilon^T \Theta \epsilon + \frac{1}{m_t} (\theta - \theta^*)^T \varphi \epsilon^T \Phi B + \frac{1}{m_t} \epsilon^T \varphi B \Delta + \frac{1}{\gamma m_t} (\theta - \theta^*)^T \dot{\theta} \\ &= -\frac{1}{2} \epsilon^T \Theta \epsilon + \frac{1}{m_t} (\theta - \theta^*)^T \left( \varphi \epsilon^T \Phi B + \frac{1}{\gamma} \dot{\theta} \right) + \frac{1}{m_t} \epsilon^T \Phi B \Delta \quad (25)\end{aligned}$$

Therefore, the weights update law

$$\dot{\theta} = -\gamma \varphi \epsilon^T \Phi B \quad (26)$$

leads to

$$\dot{L} = -\frac{1}{2} \epsilon^T \Theta \epsilon + \frac{1}{m_t} \epsilon^T \Phi B \Delta \quad (27)$$

Since  $\Theta$  is a symmetric positive definite matrix, we can easily find that  $-\frac{1}{2} \epsilon^T \Theta \epsilon$  is negative definite. The position- and the velocity-tracking error of the trolley  $\epsilon$ , and the approximation error of the PNCC  $\Delta$  can be made very small by chosen appropriate parameters  $k_p, k_d, \gamma, \Theta, \epsilon$ , and  $b$ . Therefore, we can obtain

$$\frac{1}{m_t} \epsilon^T \Phi B \Delta < \frac{1}{2} \epsilon^T \Theta \epsilon \quad (28)$$

then that the derivative  $\dot{L}$  is negative definite can be guaranteed.

In addition,  $L \rightarrow \infty$  as  $\|\epsilon\| \rightarrow \infty$  and  $\|\theta - \theta^*\| \rightarrow \infty$ , which means positive definite function  $L$  is radially unbounded. By using Theorem 3.3 (Global Stability) in [34], we then obtain that the equilibrium at the origin of  $\epsilon$  is global asymptotically stable.

## 4 | NUMERICAL SIMULATION

### 4.1 | Reference trajectory

In these simulations, the reference trajectory, which is S-shape smooth function and aims to eliminate the residual sway angle of the payload, is chosen as [16]

$$x_d(t) = \frac{p_d}{2} + \frac{k_v^2}{4k_a} \ln \left[ \frac{\cosh\left(\frac{2k_a}{k_v}t - \varepsilon\right)}{\cosh\left(\frac{2k_a}{k_v}t - \varepsilon - \frac{2k_a}{k_v^2}p_d\right)} \right] \quad (29)$$

where  $p_d$  is the desired the position, and other parameters, i.e.  $k_v, k_a$  and  $\varepsilon$ , are used to shape the trajectory.

The desired position of the trolley is chosen as

$$p_d = 20 \text{ m}$$

and the other parameters for reference trajectory (29) are chosen as

$$k_v = 3, \quad k_a = 0.5, \quad \varepsilon = 4$$

Note that, the following simulations and results analyses are based on the same reference trajectory.

### 4.2 | Simulation results

#### 4.2.1 | Comparison study

The structure of the PNCC (13) is chosen as 2-5-1, which represent the number of input-layer, hidden-layer and output-layer neurons, respectively. The NN input vector is

$$X = \epsilon^T$$

The parameters of hidden-layer radial basis functions are chosen as

$$c = [c_1, c_2, c_3, c_4, c_5] = \begin{bmatrix} -2 & -1 & 0 & 1 & 2 \\ -2 & -1 & 0 & 1 & 2 \end{bmatrix}$$

$$b = [b_1, b_2, b_3, b_4, b_5] = [20, 20, 20, 20, 20]$$

The weight between hidden layer and output layer is initialized as

$$\theta(0) = [0 \ 0 \ 0 \ 0 \ 0]^T$$

The control gains and adaptive parameters of the proposed controller are tuned empirically as

$$\begin{aligned}k_p &= 2, \quad k_d = 1, \quad \gamma = 500, \\ \Theta &= \begin{bmatrix} 40 & 000 & 0 \\ 0 & 40 & 000 \end{bmatrix}\end{aligned}$$

Note that: i) the parameters of system, i.e. trolley mass, the hook mass, the payload mass, and the cable lengths, are not given to the NN controller, and the estimation laws of these parameters are not designed, ii) the

nonlinear dynamic equations (4) of the double-pendulum crane model are implemented in these simulations, and iii) all parameters for the PNNC will not be changed among these simulations.

For a comparison study, an Adaptive Hierarchical Sliding Mode Control(AHSMC) [35] is selected. The control law of the AHSMC is written as

$$u = -\frac{\hat{\lambda}_3(\dot{x} - \dot{x}_d + \lambda_1\dot{\alpha} + \lambda_2\dot{\beta})}{b_1 + \lambda_1b_2 + \lambda_2b_3} - \frac{\kappa s + \eta \tanh(s)}{b_1 + \lambda_1b_2 + \lambda_2b_3} \quad (30)$$

where  $\lambda_1, \lambda_2, \kappa$  and  $\eta$  are positive constants selected by trial and error method.  $\lambda_3$  is a time-varying parameter with an adaptation law

$$\dot{\lambda}_3 = -\frac{s_2(d_1 + \lambda_1d_2 + \lambda_2d_3 - \ddot{x}_d)}{s_2^2 + \delta}$$

where  $\delta$  is a positive constant.  $s$  and  $s_2$  are sliding surfaces, and  $b_1, b_2, b_3, d_1, d_2$  and  $d_3$  are defined as

$$b_i \triangleq F_i(m_t, m_h, m_p, l_1, l_2, \alpha, \beta), i = 1, 2, 3$$

$$d_i \triangleq H_i(m_t, m_h, m_p, l_1, l_2, \alpha, \beta, \dot{\alpha}, \dot{\beta}), i = 1, 2, 3$$

As mentioned before in Section 2, the friction force, as well as the air resistance are ignored. In these simulations, the nominal values of the trolley mass, the hook mass, the payload mass, and the cable lengths, which are inputted to the adaptive controller (30), are the actual values. For more details about the AHSMC, please refer to [35].

The control gains  $\lambda_1, \lambda_2, \kappa, \eta$ , and  $\delta$  are tuned carefully as follow

$$\lambda_1 = 0.01, \lambda_2 = 0.01, \kappa = 200, \eta = 0.03, \delta = 0.5$$

In this paper, the trolley mass and the hook mass, which are considered as constant values, are chosen as

$$m_t = 2000 \text{ kg}, m_h = 100 \text{ kg}$$

The following 2 cases are considered for a comparison study.

**Case I.**  $m_p=100 \text{ kg}, l_1=1.5 \text{ m}, l_2=1 \text{ m}$

**Case II.**  $m_p=1000 \text{ kg}, l_1=1.5 \text{ m}, l_2=1 \text{ m}$

Zero initial states are considered in these simulations. The simulation results are shown in Figures 3–6.

From Figure 3 and 4, it can be found that the position tracking errors of both the PNNC and the AHSMC are eventually reduce to 0. The position tracking errors of the PNNC are nearly 0 (no more than 0.0015 m), while the maximums of the position tracking errors of the AHSMC are approximate 0.0174 m and 0.1319 m in Case I and II, respectively. Therefore, the PNNC has more robust tracking performance than the AHSMC in these cases.

From Figure 5 and 6, it can be found that the control force of the PNNC are less than that of the AHSMC, and the PNNC costs less time to stabilize the payload to a steady state. In Figure 5, it shows that both the PNNC and the AHSMC achieve perfect performance of eliminating the residual sway of the hook and the payload under light load condition ( $m_p=100 \text{ kg}$ ). In Figure 6, it shows that the PNNC maintains the sway eliminating performance as its tracking error keeps the same, but the AHSMC does not achieve the goal of eliminating the sway angles. The maximum residual sway angles of the hook and the payload are  $0.6040^\circ$  and  $0.6268^\circ$ , respectively. More details of the comparison study are listed in Table 1. The setting time means that, from this moment on (to the end of the simulation), the sway angles of the

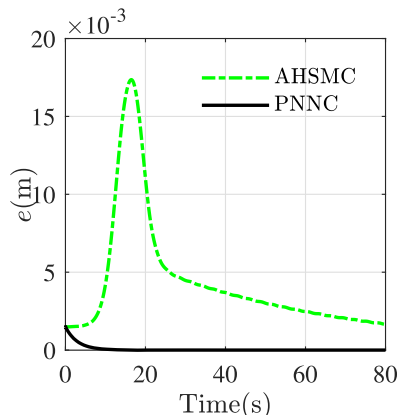
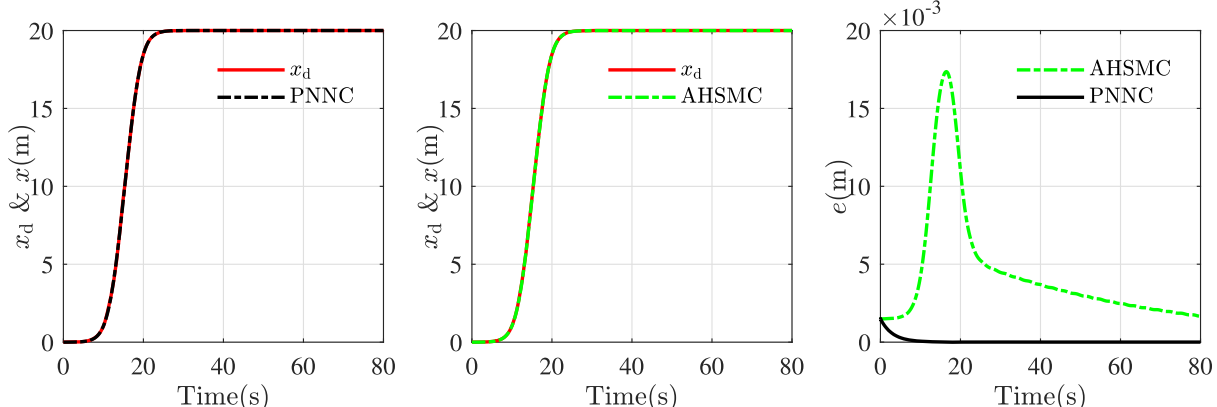


**FIGURE 3** Position tracking results: **Case I** [Color figure can be viewed at [wileyonlinelibrary.com](http://wileyonlinelibrary.com)]

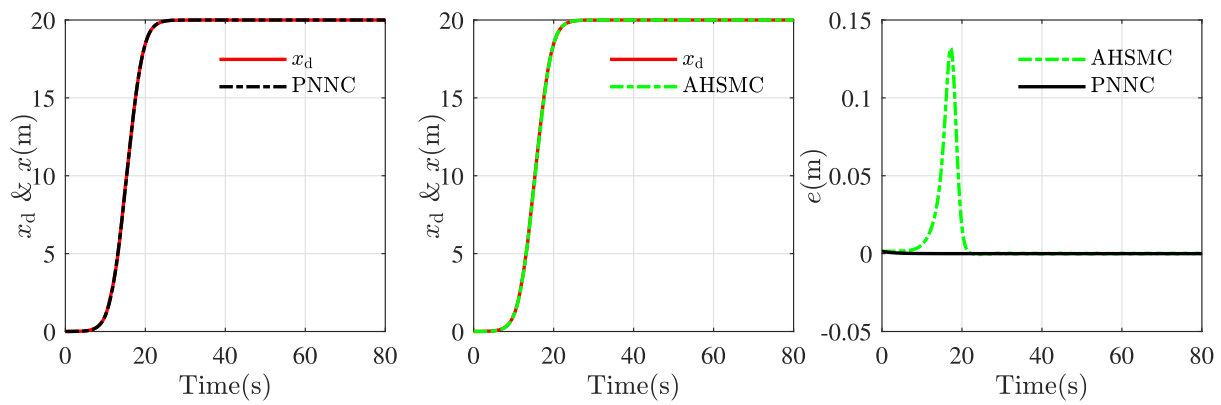


**FIGURE 4** Position tracking results: **Case II** [Color figure can be viewed at [wileyonlinelibrary.com](http://wileyonlinelibrary.com)]

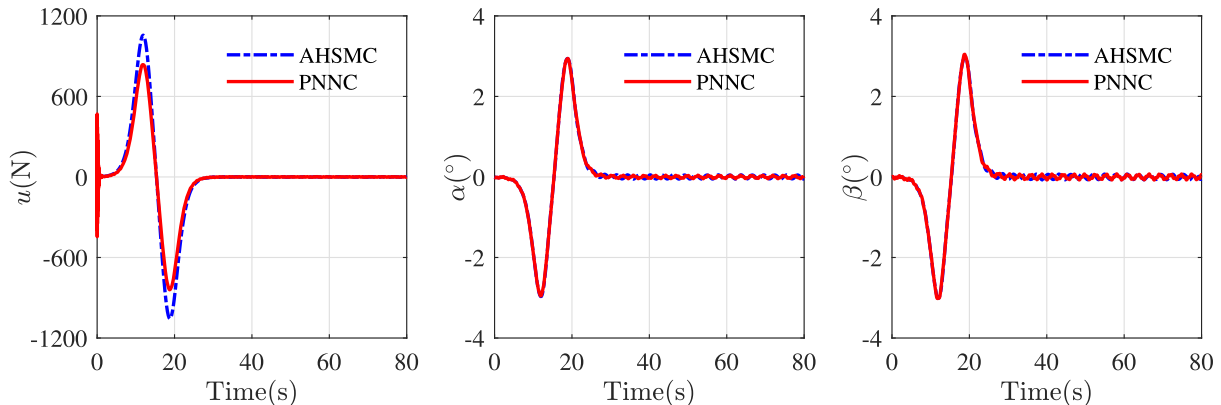


**FIGURE 5** Control force and sway angles: **Case I** [Color figure can be viewed at [wileyonlinelibrary.com](http://wileyonlinelibrary.com)]

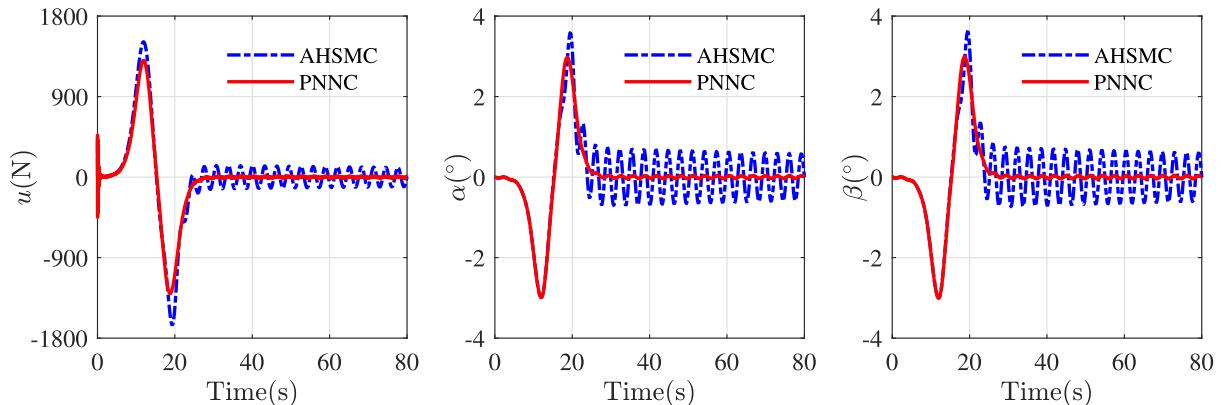


**FIGURE 6** Control force and sway angles: **Case II** [Color figure can be viewed at [wileyonlinelibrary.com](http://wileyonlinelibrary.com)]

hook and the payload belong to  $(-0.1^\circ, 0.1^\circ)$ . Note that the control gains of both the AHSMC and the PNNC are not changed in this section.

In summary, we can summarize the main advantages of the PNNC compared to the AHSMC as follows:

1. the PNNC has a simple form (13), while the AHSMC has a complex one (30).

2. the PNNC is a model-free controller, i.e. the information of system parameters is not needed, while the AHSMC needs the actual values of all system parameters.
3. the PNNC requires partial feedback signals, i.e. the position and the velocity signals of the trolley, while the AHSMC requires full states feedback. Note that in the practical application, the sway angles of the

**TABLE 1** Comparison study

Case	Controller	$ u _{\max}(N)$	$ e _{\max}(m)$	$ \alpha _{\max}(\text{deg})$	$ \alpha _{\text{res}}(\text{deg})$	$ \beta _{\max}(\text{deg})$	$ \beta _{\text{res}}(\text{deg})$	setting time(s)
Case I	PNNC	840.26	0.0015	2.96	0.0444	3.05	0.0756	25.59
	AHSMC	1056.60	0.0174	2.97	0.0519	3.02	0.0702	26.15
Case II	PNNC	1305.28	0.0015	2.99	0.0396	3.01	0.0444	26.39
	AHSMC	1653.68	0.1319	3.59	0.6040	3.62	0.6268	80.00

<sup>a</sup> $|\alpha|_{\text{res}}$  and  $|\beta|_{\text{res}}$  mean the amplitude of the residual sway angle of the hook and the payload, respectively.

hook and the payload are difficult to measure fast and accurately online. Therefore, it is difficult for AHSMC to implement in the real world.

4. the PNNC has more robust tracking performance than the AHSMC, so it leads to the PNNC has better sway eliminating performance than the AHSMC.

#### 4.2.2 | Robustness and Analysis

In this section, the PNNC's sensitivity to the variation of the payload mass and cable lengths are studied. The double-pendulum crane system is considered as zero initial states in this section, too. The control parameters of

the PNNC remain the same. The trolley mass and the hook mass remain as

$$m_t = 2000 \text{ kg}, m_h = 100 \text{ kg}$$

and we add the following 4 cases for comparison:

**Case A.**  $m_p = 100 \text{ kg}, l_1 = 1 \text{ m}, l_2 = 1 \text{ m}$

**Case B.**  $m_p = 100 \text{ kg}, l_1 = 1 \text{ m}, l_2 = 1.5 \text{ m}$

**Case C.**  $m_p = 1000 \text{ kg}, l_1 = 1 \text{ m}, l_2 = 1 \text{ m}$

**Case D.**  $m_p = 1000 \text{ kg}, l_1 = 1 \text{ m}, l_2 = 1.5 \text{ m}$

Figure 7 presents the light load condition ( $m_p=100 \text{ kg}$ ). The residual sway of both the hook and the payload are

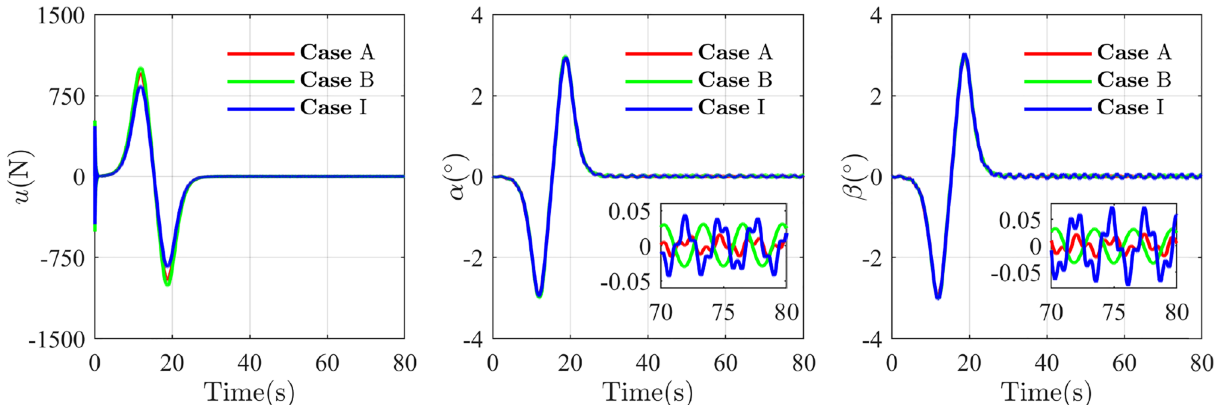


**FIGURE 7** Simulation results: Case A, B, and I [Color figure can be viewed at [wileyonlinelibrary.com](http://wileyonlinelibrary.com)]

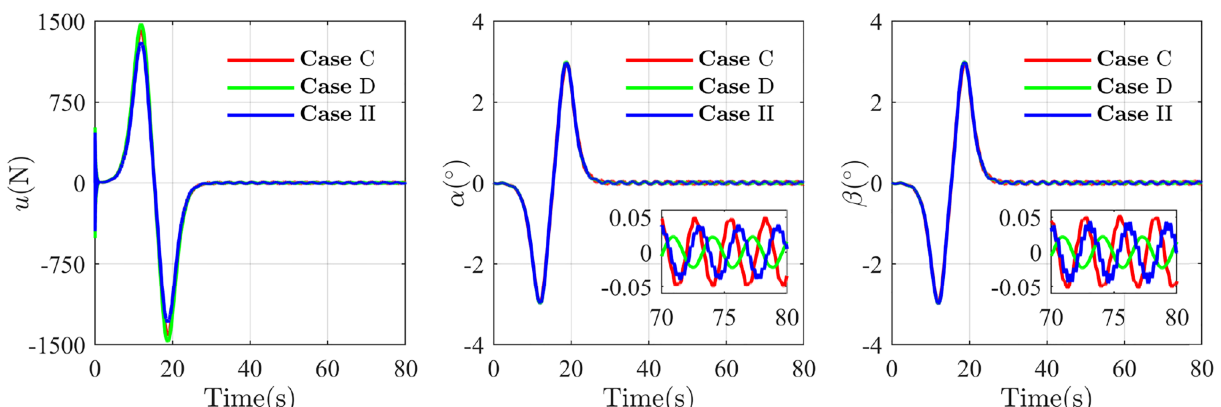


**FIGURE 8** Simulation results: Case C, D, and II [Color figure can be viewed at [wileyonlinelibrary.com](http://wileyonlinelibrary.com)]

**TABLE 2** Robustness study

Case	$ u _{\max}(\text{N})$	$ e _{\max}(\text{m})$	$ \alpha _{\max}(\text{deg})$	$ \alpha _{\text{res}}(\text{deg})$	$ \beta _{\max}(\text{deg})$	$ \beta _{\text{res}}(\text{deg})$	setting time(s)
Case A	958.16	0.0015	2.92	0.0162	2.97	0.0230	25.74
Case B	1011.27	0.0015	3.00	0.0312	3.01	0.0336	25.32
Case I	840.26	0.0015	2.96	0.0444	3.05	0.0756	25.59
Case C	1418.33	0.0015	2.98	0.0501	2.99	0.0524	25.68
Case D	1474.34	0.0015	3.01	0.0224	3.01	0.0225	25.39
Case II	1305.28	0.0015	2.99	0.0396	3.01	0.0444	26.39

less than  $0.1^\circ$ . It shows that the residual sways with larger  $l_1$  (**Case D**) or  $l_2$  (**Case II**) are slightly greater than that with smaller cable length (**Case C**). Figure 8 presents the heavy load condition ( $m_p=1000 \text{ kg}$ ). It can be found that the residual sway of the hook and that of the payload change little when  $l_1$  is not changed (in **Case A** and **B**,  $l_1=1 \text{ m}$ ).

In these simulations, all the tracking results of the trolley the position are shown in Table 2. The tracking error  $e$  is no more than 0.0015 m. It can be found, under the control of the PNCC, the changes of the payload mass and cable lengths have little effect on the position tracking of the trolley. In other words, the proposed PNCC is robust to the variation of system parameters, i.e. the payload mass and cable lengths.

## 5 | CONCLUSION

In this paper, based on the Lyapunov stability theory, we proposed a pure neural network controller, whose weights are updated online, and it is used to anti-sway control for crane systems by tracking the ideal trajectory of the trolley. As the controller is model-free, the estimation laws to identify the system parameters are not required. Thus, it is robust to the variation of system parameters and reduces the computational effort. The proposed controller has excellent tracking performance, and the goal of eliminating the residual sways can be achieved when the ideal trajectory of the trolley is carefully designed. The proposed controller only requires the output feedback signals of the trolley, i.e. the position and the velocity of the trolley. Therefore, it can be implemented on single-pendulum cranes as well. However, as a coin has two sides, on one hand, if the crane runs indoors (without wind disturbance), it saves costs without the payload sway measuring equipment; on the other hand, if the crane runs outdoors (with wind disturbance), the goal of eliminating the payload residual sway may not be achieved without feedback signals of the sway angles of the hook and the payload. In our future work, the wind disturbance induced sway issue and the actuator

nonlinearities will be considered important research directions, and it will be interesting to extend the proposed controller to solve the regulation problems if all states are available and to extend the proposed controller to solve the tracking control issues of other linear/nonlinear systems, such as boom cranes, tower cranes, and other full-actuated/under-actuated systems.

## ACKNOWLEDGMENTS

This paper is funded by the Sichuan Science and Technology Program (No. 2019YFG0300, No. 2019YFG0285). The first author received a one-year scholarship from the China Scholarship Council (No. 201807000126). The first author would also like to thank Dr. Du Run and Mr. Li Fei for their advice.

## ORCID

Qingrong Chen  <https://orcid.org/0000-0002-2780-4258>

## REFERENCES

- W. Singhose, *Command shaping for flexible systems: A review of the first 50 years*, Int. J. Precis. Eng. Manuf. **10** (2009), no. 4, 153–168. <https://doi.org/10.1007/s12541-009-0084-2>
- J. Vaughan, D. Kim, and W. Singhose, *Control of tower cranes with double-pendulum payload dynamics*, IEEE Trans. Control Syst. Technol. **18** (2010), no. 6, 1345–1358. <https://doi.org/10.1109/TCST.2010.2040178>
- D. Fujioka and W. Singhose, *Optimized input-shaped model reference control on double-pendulum system*, J. Dyn. Syst. Meas. Control. **140** (2018), no. 10, 101004. <https://doi.org/10.1115/1.4039786>
- K. L. Sorensen, W. Singhose, and S. Dickerson, *A controller enabling precise positioning and sway reduction in bridge and gantry cranes*, Control Eng. Pract. **15** (2007), no. 7, 825–837.
- R. Mar et al., *Combined input shaping and feedback control for double-pendulum systems*, Mech. Syst. Sig. Process. **85** (2017), 267–277. <https://doi.org/10.1016/j.ymssp.2016.08.012>
- H. I. Jaafar et al., *Model reference command shaping for vibration control of multimode flexible systems with application to a double-pendulum overhead crane*, Mech. Syst. Sig. Process. **115** (2019), 677–695. <https://doi.org/10.1016/j.ymssp.2018.06.005>

7. M. J. Maghsoudi et al., *Improved unity magnitude input shaping scheme for sway control of an underactuated 3D overhead crane with hoisting*, *Mech. Syst. Sig. Process.* **123** (2019), 466–482. <https://doi.org/10.1016/j.ymssp.2018.12.056>
8. B. Lu, Y. Fang, and N. Sun, *Enhanced-coupling adaptive control for double-pendulum overhead cranes with payload hoisting and lowering*, *Automatica* **101** (2019), 241–251. <https://doi.org/10.1016/j.automatica.2018.12.009>
9. N. Sun et al., *Nonlinear antiswing control for crane systems with double-pendulum swing effects and uncertain parameters: Design and experiments*, *IEEE Trans. Autom. Sci. Eng.* **15** (2018), no. 3, 1413–1422. <https://doi.org/10.1109/TASE.2017.2723539>
10. M. Zhang et al., *Nonlinear coupling control method for underactuated three-dimensional overhead crane systems under initial input constraints*, *Trans. Inst. Meas. Control* **40** (2018), no. 2, 413–424. <https://doi.org/10.1177/0142331216658949>
11. L. A. Tuan and S.-G. Lee, *Sliding mode controls of double-pendulum crane systems*, *J. Mech. Sci. Technol.* **27** (2013), no. 6, 1863–1873. <https://doi.org/10.1007/s12206-013-0437-8>
12. N. Sun et al., *Amplitude-saturated nonlinear output feedback antiswing control for underactuated cranes with double-pendulum cargo dynamics*, *IEEE Trans. Ind. Electron.* **64** (2017), no. 3, 2135–2146. <https://doi.org/10.1109/TIE.2016.2623258>
13. M. Zhang et al., *A novel energy-coupling-based control method for double-pendulum overhead cranes with initial control force constraint*, *Adv. Mech. Eng.* **10** (2018), no. 1, 1–13. <https://doi.org/10.1177/1687814017752213>
14. N. Sun et al., *Transportation control of double-pendulum cranes with a nonlinear quasi-pid scheme: Design and experiments*, *IEEE Trans. Syst. Man Cybern: Syst.* **49** (2018), no. 7, 1408–1418. <https://doi.org/10.1109/TSMC.2018.2871627>
15. Q. H. Ngo et al., *Payload pendulation and position control systems for an offshore container crane with adaptive-gain sliding mode control*, *Asian J. Control* (2019), 1–10. <https://doi.org/10.1002/asjc.2124>
16. M. Zhang et al., *Adaptive tracking control for double-pendulum overhead cranes subject to tracking error limitation, parametric uncertainties and external disturbances*, *Mech. Syst. Sig. Process.* **76–77** (2016), 15–32. <https://doi.org/10.1016/j.ymssp.2016.02.013>
17. H. Ouyang et al., *Decoupled linear model and S-shaped curve motion trajectory for load sway reduction control in overhead cranes with double-pendulum effect*, *Proc. IME C. J. Mech. Eng. Sci.* **233** (2019), no. 10, 3678–3689. <https://doi.org/10.1177/0954406218819029>
18. S. U. Choi et al., *A study on gantry crane control using neural network two degree of PID controller*, *2001 IEEE International Symposium on Industrial Electronics Proceedings*, Vol. 3. IEEE, Pusan, South Korea, 2001, pp. 1896–1900.
19. J.-H. Suh et al., *Anti-sway position control of an automated transfer crane based on neural network predictive PID controller*, *J. Mech. Sci. Technol.* **19** (2005), no. 2, 505–519. <https://doi.org/10.1007/BF02916173>
20. H. Saeidi, M. Naraghi, and A. A. Raie, *A neural network self tuner based on input shapers behavior for anti sway system of gantry cranes*, *J. Vib. Control.* **19** (2013), no. 13, 1936–1949. <https://doi.org/10.1177/1077546312453065>
21. H. I. Jaafar et al., *Efficient control of a nonlinear double-pendulum overhead crane with sensorless payload motion using an improved PSO-tuned PID controller*, *J. Vib. Control.* **25** (2019), no. 4, 907–921. <https://doi.org/10.1177/1077546318804319>
22. M. A. Shehu et al., *Comparative analysis of neural-network and fuzzy auto-tuning sliding mode controls for overhead cranes under payload and cable variations*, *J. Control Sci. Eng.* (2019), 1–13. <https://doi.org/10.1155/2019/1480732>
23. X. Shao, J. Zhang, and X. Zhang, *Takagi-sugeno fuzzy modeling and pso-based robust LQR anti-swing control for overhead crane*, *Math. Probl. Eng.* **2019** (2019), 1–14. <https://doi.org/10.1155/2019/4596782>
24. L.-H. Lee et al., *Parallel neural network combined with sliding mode control in overhead crane control system*, *J. Vib. Control.* **20** (2014), no. 5, 749–760. <https://doi.org/10.1177/1077546314464681>
25. S. Frikha, M. Djemel, and N. Derbel, *A new adaptive neuro-sliding mode control for gantry crane*, *Int. J. Control. Autom. Syst.* **16** (2018), no. 2, 559–565. <https://doi.org/10.1007/s12555-017-0070-x>
26. J. Matuško, Š. Ilješ, F. Kolonić, and V. Lešić, *Control of 3d tower crane based on tensor product model transformation with neural friction compensation*, *Asian J. Control* **17** (2015), no. 2, 443–458. <http://doi.org/10.1002/asjc.986>
27. J. Liu, *Radial Basis Function (RBF) Neural Network Control for Mechanical Systems: Design, Analysis and MATLAB Simulation*, Springer, Berlin, Heidelberg, 2013.
28. Z. Yan, M. Wang, and J. Xu, *Global adaptive neural network control of underactuated autonomous underwater vehicles with parametric modeling uncertainty*, *Asian J. Control* **21** (2019), no. 4, 1–13. <https://doi.org/10.1002/asjc.1819>
29. G. Zhang and X. Zhang, *Practical robust neural path following control for underactuated marine vessels with actuators uncertainties*, *Asian J. Control* **19** (2017), no. 1, 173–187. <https://doi.org/10.1002/asjc.1345>
30. T. Yang et al., *Neural network-based adaptive antiswing control of an underactuated ship-mounted crane with roll motions and input dead zones*, *IEEE Trans. Neural Netw. Learn. Syst.* (2019), 1–14. <https://doi.org/10.1109/TNNLS.2019.2910580>
31. H. Yang and J. Liu, *An adaptive RBF neural network control method for a class of nonlinear systems*, *IEEE/CAA Journal of Automatica Sinica* **5** (2018), no. 2, 457–462. <https://doi.org/10.1109/JAS.2017.7510820>
32. Z. N. Masoud and A. H. Nayfeh, *Sway reduction on container cranes using delayed feedback controller*, *Nonlinear Dyn.* **34** (2003), no. 3–4, 347–358.
33. Z. N. Masoud, A. H. Nayfeh, and N. A. Nayfeh, *Sway reduction on quay-side container cranes using delayed feedback controller: Simulations and experiments*, *J. Vib. Control* **11** (2005), no. 8, 1103–1122. <https://doi.org/10.1177/1077546305056300>
34. J.-J. E. Slotine and W. Li, *Applied Nonlinear Control*, Prentice Hall, Englewood Cliffs, NJ, 1991.
35. H. Ouyang et al., *Novel adaptive hierarchical sliding mode control for trajectory tracking and load sway rejection in double-pendulum overhead cranes*, *IEEE Access* **7** (2019), 10353–10361. <https://doi.org/10.1109/ACCESS.2019.2891793>

**AUTHOR BIOGRAPHIES**

**Qingrong Chen** received his B.S. degree in mechanical design, manufacturing and automation from Southwest Jiaotong University, Chengdu, China, in 2015. From 2015 to now, he is an Integrated Ph.D. student in mechatronic engineering under the supervision of Prof. Dr. Wenming Cheng at Southwest Jiaotong University, Chengdu, China. From 2018 to now, he is also a visiting Ph.D. student under the supervision of Prof. Dr. Johannes Fottner at Technical University of Munich, Munich, Germany. His research interests include dynamics analysis and intelligent control of crane systems.



**Wenming Cheng** received the B.S. degree in hoisting and conveying machinery from Southwest Jiaotong University, Chengdu, China, in 1984, the M.S. degree in engineering machinery and Ph.D. degree in mechanical design and theory from the same university in 1989 and in 2000, respectively. He is currently a Professor with the School of Mechanical Engineering, Southwest Jiaotong University, Chengdu, China, and the Technology and Equipment of Rail Transit Operation and Maintenance Key Laboratory of Sichuan Province, Chengdu, China. He is also the Director of the Department of Engineering Machinery, School of Mechanical Engineering, Southwest Jiaotong University, Chengdu, China. His research interests include the basic theory and design of engineering machinery and logistics engineering.



**Lingchong Gao** received his B.S. degree in logistic engineering from Dalian University of Technology, Dalian, China, in 2012 and his M.S. degree in machinery design and theory from Dalian University of Technology, Dalian, China, in 2015. From 2015 to now, he works as a scientific assistant and pursues his doctorate at the Chair of Materials Handling, Material

Flow, Logistics, Technical University of Munich, Munich, Germany. His research interests include the dynamic simulation and analysis of multi-domain mechanical system. Especially the long boom manipulator system of mobile cranes and aerial platform vehicles which includes flexible boom structure and hydraulic drive system.



**Johannes Fottner** studied mechanical engineering at Technical University of Munich, Munich, Germany and received his Dr.-Ing. degree at the same university in the field of materials handling, material flow and logistics. From 2002 to 2008, he held a number of managerial positions at the Swisslog Group. In 2008, he took over as managing director of the MIAS Group. Fottner holds the Bavarian state chair and national deputy chair of the Society for Production and Logistics at the Association of German Engineers (VDI). In 2016, he was appointed as the professor of logistics engineering at Technical University of Munich, Munich, Germany. His research work focuses on several central topics of technical logistics, especially new technical solutions and systems approaches to improve logistical processes, he also places a special emphasis on practical applications of scientific knowledge.

**How to cite this article:** Chen Q, Cheng W, Gao L, Fottner J. A pure neural network controller for double-pendulum crane anti-sway control: Based on Lyapunov stability theory. *Asian J Control*. 2019;1–12. <https://doi.org/10.1002/asjc.2226>